Particle Accelerators, 1990, Vol. 34, pp. 105–126
Reprints available directly from the publisher
Photocopying permitted by license only

BUNCHED-BEAM LONGITUDINAL MODE-COUPLING AND ROBINSON-TYPE INSTABILITIES*

TAI-SEN F. WANG

AT-6, MS H829, Los Alamos National Laboratory, Los Alamos, NM 87545, USA

(Received April 5, 1989)

Using Sacherer's integral equation, Robinson's stability conditions are re-derived by considering the coupling between the upper and lower synchrotron sidebands at the rf frequency. The equivalent circuit model approach and the kinetic description provide almost the same results except for a factor that depends on the equilibrium phase-space distribution of beam particles. The stability threshold current derived from the Vlasov equation is shown to be higher than Robinson's stability limit. The coupling between the longitudinal dipole and the quadrupole modes is also studied for a bunched beam under the influence of a resonator impedance. In the small cavity-detuning region, Robinson's stability limit is substantially modified by the coupling between dipole and quadrupole modes.

1. INTRODUCTION

The stability of a beam-cavity interaction system has been of interest in both accelerator design and the academic study of beam dynamics since the initial work by K. W. Robinson in the middle 1950s.[1,2] For a synchrotron or a storage ring operated below transition, Robinson showed that the stability conditions are

$$0 < \sin(2\phi_y), \tag{1}$$

and

$$I_b < \frac{2V_m \cos\psi_s}{\mathcal{R}\sin(2\phi_y)}, \tag{2}$$

where

$$\phi_y = \tan^{-1}\frac{2Q(\omega_R - \omega_{RF})}{\omega_R} \tag{3}$$

is the rf detuning angle, Q is the quality factor of the cavity, ω_R is the resonant frequency of the cavity, ω_{RF} is the frequency of the applied rf power, I_b is approximately equal to the Fourier component of the beam current at the rf frequency, V_m is the maximum voltage on the cavity, ψ_s is the synchronous angle between the beam current and the voltage on the cavity, and $\mathcal{R}$ is the shunt resistance of the cavity. For machines operated above transition, the inequality sign in Inequality (1) needs to be reversed. Inequality (1), to be referred to as

* Work supported by Los Alamos National Laboratory Institutional Supporting Research, under the auspices of the United States Department of Energy.

Robinson's first criterion in the following, defines the stability range that the frequency of the rf power can be detuned from the resonant frequency of the cavity. Inequality (2), hereinafter called *Robinson's second criterion,* shows the relation among the synchronous angle, the cavity detuning, and the stable beam current that can be stored or accelerated. For narrow-band cavities, short beam bunches, and large detuning angles, Robinson's criteria provide simple-to-use relations and results accurate enough for estimation purposes (see the discussions below). We notice that the first criterion is independent of the beam current and the second criterion indicates that the maximum stable beam current approaches infinity when the detuning angle approaches zero.

Robinson's stability conditions were originally derived by using an equivalent circuit model for the beam-cavity system before the more elaborate theory of bunched-beam stability was formulated based on the Vlasov equation of the kinetic description.[3–6] After Robinson's work, the same or similar problems were examined by using approaches and formalisms other than the equivalent circuit model, including the use of the Vlasov equation.[3,7–24] One of the advantages of using the Vlasov equation over the equivalent circuit model is that higher synchrotron harmonics are included in the formalism in a natural way, while the equivalent circuit approach has to include these harmonics in an *ad hoc* manner. In general, there is no unique procedure or formalism for applying the Vlasov equation to derive the stability information, but a widely used formalism was developed by Lebedev and Sacherer.[3,4] In Sacherer's formalism, an integral equation is deduced from the linearized Vlasov equation to describe the behavior of small longitudinal perturbations in a bunched beam, and the perturbations of the beam-particle distribution in phase space are categorized according to the harmonics of the synchrotron frequency. Because the synchrotron frequency is usually much lower than the fundamental frequency of an rf cavity, synchrotron harmonics may appear in the beam signal as sidebands around the rf frequency. For narrow-band resonators, only those synchrotron sidebands near the resonant frequencies of the cavity contribute significantly to the beam-cavity interaction. For a beam with more than one bunch, the content of Robinson's stability covers only the *coherent* motions of dipole modes among bunches. The *coupled bunch modes* that are caused by the relative motions among bunches are not included. Yet, even within the category of coherent motion, more than just the dipole mode is important. The term "Robinson-Type Instability" is used in this paper to mean the instability of the coherent bunch mode that may include any possible coupling among synchrotron harmonics.

The equivalent circuit analysis has shown that the Robinson instability is due to the coupling of the upper and lower synchrotron sidebands next to the rf frequency and the effect of the frequency dependence of the cavity impedance. All these factors causing the instability can be included in any formalism based on the Vlasov equation. Nevertheless, among the publications using the Vlasov equation, only Robinson's first criterion has been reproduced explicitly, while a re-derivation of the second criterion by this technique still has not been seen in the literature. Even very recently, the consistency between the use of the equivalent circuit model and the use of Sacherer's integral equation for examining the stability of the beam-cavity system is still being questioned.[23] In fact, a dispersion relation, similar to the fourth-order algebraic equation originally derived by Robinson, was obtained by Gumoski by using the Vlasov equation in a formalism different from Sacherer's.[11] However, instead of re-examining the Robinson instability, the author was interested in the numerical solutions of the more general dispersion relation for the relatively wide-band resonator impedance.

Because of practical importance and mathematical simplicity, the stability of the dipole modes has been extensively studied. As will be shown later, for a tightly bunched beam interacting with a highly or moderately detuned narrow-band resonator, the neglect of higher synchrotron harmonics is a good approximation. However, for long beam bunches or small cavity detuning, higher synchrotron harmonics may affect the stability appreciably; therefore, at least a few of the higher synchrotron harmonics should be considered. When more synchrotron harmonics are included, the mathematics involved in solving the Vlasov equation becomes difficult except for a few special equilibrium phase-space distributions.[19] The customary stability study for a multimode problem is either to use computer simulation or to apply the Vlasov equation and then use numerical calculation to examine the roots of the dispersion relation for specific cases.[20–22,24] These kinds of approaches seem to be the only practical ones if wide-band impedances are considered. Nonetheless, mathematical experiments have shown that if only a few modes are coupled, the analytical calculation may still be manageable and some general but simple stability conditions can be derived. The results might not be completely accurate but can still show how the single-mode conclusions are modified qualitatively.

The purposes of this paper are twofold. The first purpose is to show that if the dipole mode is the only mode under consideration, the result obtained from the equivalent circuit model approach agrees very well with the result derived from the kinetic description except for a factor that depends on the phase-space distribution of beam particles. The second purpose is to study the effects of the coupling between the dipole and the quadrupole modes for a narrow-band resonator impedance. In the next section, we shall present the details of the derivation of Robinson's stability conditions by using Sacherer's integral equation. The coupling between dipole and quadrupole modes will be studied in Section 3. For simplicity, we limit our study here to the Robinson-type instability of a multibunch system, i.e., the coupled-bunch modes are not considered here. We shall concentrate on the case below transition. Above transition, the analysis is similar. For comparison, the derivation of Robinson's stability conditions from the equivalent circuit formalism is included as Appendix A.

2. ROBINSON'S STABILITY CRITERIA RE-DERIVED

Consider the case of M equally spaced particle bunches circulating with angular revolution-frequency Ω_0 in a circular accelerator or a storage ring. We choose a coordinate system such that the z-axis is along the direction of particle propagation. For the purpose of our discussion, we can neglect the repulsive Coulomb force between particles in the equilibrium state, although we consider the Coulomb force resulting from the density perturbations. Thus, the bunch equilibrium is maintained by balancing the kinetic pressure and the rf focusing. We assume that the rf focusing experienced by a beam particle can be approximated by a linear function of the distance extended from the center of each bunch, i.e., $-\omega_s^2 z$, with the synchrotron frequency ω_s defined according to

$$\omega_s^2 = -\frac{q\eta h V_m \cos\psi_s}{2\pi m_0 \gamma R^2}, \tag{4}$$

where q and m_0 are the charge and the rest mass of a beam particle, respectively; h is the rf harmonic number; γ is the ratio between the relativistic mass and the rest mass of a beam particle; R is the effective machine radius; and

$$\eta = \frac{1}{\gamma_t^2} - \frac{1}{\gamma^2} \tag{5}$$

is the momentum slip factor for a machine with transition energy $m_0 c^2 \gamma_t$. The single-particle orbit then is given by

$$z = r\cos(\omega_s t + \theta), \tag{6}$$

and

$$v_z = -\omega_s r \sin(\omega_s t + \theta), \tag{7}$$

where v_z is the velocity of the particle relative to the reference particle at the bunch center, θ is the phase angle depending on the initial condition, and

$$r = \sqrt{z^2 + (v_z/\omega_s)^2} \tag{8}$$

is the ampliutde of the synchrotron oscillation of the particle. We assume that all bunches have the same equilibrium particle distribution described by a distribution function $f_0(z, v_z)$ in the phase space. Neglecting the relative motion among bunches, the following Sacherer's integral equation for the *coherent modes* of longitudinal perturbations can be derived from the linearized Vlasov equation:[6,21]

$$(\omega - l\omega_s)R_l(r) = \frac{q^2 M\eta\Omega_0 l}{2\pi m_0 \gamma r}\left(\frac{df_0}{dr}\right)\sum_{n,m}\frac{Z_n(\omega + n\Omega_0)}{n} i^{m-l-1} \times J_l\left(\frac{nr}{R}\right)\int_0^\infty R_m(r')J_m\left(\frac{nr'}{R}\right)r'\,dr', \tag{9}$$

where r has been defined in Eq. (8), ω is the frequency to be solved, l is an integer designating the azimuthal harmonics of the perturbation in the phase space of an individual bunch, $R_l(r)$ is the Fourier content of the lth harmonic of the perturbation in the phase space, n is the azimuthal harmonic number around the ring, $Z_n(\omega + n\Omega_0)$ is the longitudinal impedance at the frequency $\omega + n\Omega_0$, and $J_k(x)$ is the kth order Bessel function of the first kind with argument x. In arriving at Eq. (9), we have assumed that the equilibrium distribution function depends on r only, and we have neglected the *time-of-flight* effect.[25]

For a narrow-band resonator impedance, we need only to consider those frequencies very close to the resonant frequency. Thus, we need only to consider the cases of $n = \pm h$, $l = \pm 1$, and $m = \pm 1$; Eq. (9) is then reduced to

$$(\omega - \omega_s)R_1(r) = -\frac{iA}{r}\left(\frac{df_0}{dr}\right)J_1\left(\frac{hr}{R}\right)[Z_h(\omega + h\Omega_0) - Z_{-h}(\omega - h\Omega_0)](\Gamma_1 - \Gamma_{-1}), \quad (10)$$

and

$$(\omega + \omega_s)R_{-1}(r) = -\frac{iA}{r}\left(\frac{df_0}{dr}\right)J_{-1}\left(\frac{hr}{R}\right)[Z_h(\omega + h\Omega_0) - Z_{-h}(\omega - h\Omega_0)](\Gamma_1 - \Gamma_{-1}), \quad (11)$$

where

$$A = \frac{q^2 M\eta\Omega_0}{2\pi h m_0 \gamma}, \quad (12)$$

and

$$\Gamma_m = \int_0^\infty R_m(r)J_m\left(\frac{hr}{R}\right)r\,dr. \quad (13)$$

Multiplying both sides of Eq. (10) by $rJ_1(hr/R)$ and integrating over r, we have

$$(\omega - \omega_s)\Gamma_1 = -i\vartheta_1\mathscr{Z}_-(\omega)(\Gamma_1 - \Gamma_{-1}), \quad (14)$$

where

$$\vartheta_m = A\int_0^\infty \left[J_m\left(\frac{hr}{R}\right)\right]^2 \frac{df_0}{dr}\,dr, \quad (15)$$

and

$$\mathscr{Z}_-(\omega) = Z_h(\omega + h\Omega_0) - Z_{-h}(\omega - h\Omega_0). \quad (16)$$

Similarly, we can derive from Eq. (11) that

$$(\omega + \omega_s)\Gamma_{-1} = -i\vartheta_1\mathscr{Z}_-(\omega)(\Gamma_1 - \Gamma_{-1}). \quad (17)$$

For nontrivial solutions of Γ_1 and Γ_{-1}, we must have that

$$\begin{vmatrix} \omega - \omega_s + i\vartheta_1\mathscr{Z}_-(\omega) & -i\vartheta_1\mathscr{Z}_-(\omega) \\ i\vartheta_1\mathscr{Z}_-(\omega) & \omega + \omega_s - i\vartheta_1\mathscr{Z}_-(\omega) \end{vmatrix} = 0, \quad (18)$$

which is

$$\omega^2 - \omega_s^2 + 2i\vartheta_1\omega_s\mathscr{Z}_-(\omega) = 0. \quad (19)$$

To make it easy to examine the roots of the dispersion relation and to compare the derivation here with the Laplace transformation approach used in the equivalent circuit model formalism, we make a change of variable

$$s = -i\omega \quad (20)$$

in Eq. (19) to obtain

$$s^2 + \omega_s^2 - 2i\vartheta_1\omega_s\mathscr{Z}_-(\omega) = 0. \quad (21)$$

For a given impedance, if the real parts of all the roots of Eq. (21) are equal to or less than zero, then the system is stable; otherwise, there is an instability.

Now consider the narrow-band resonator impedance

$$Z_h(\omega + h\Omega_0) = \mathcal{R}\Big/\left[1 + iQ\left(\frac{\omega_R}{\omega + h\Omega_0} - \frac{\omega + h\Omega_0}{\omega_R}\right)\right],$$

$$\approx \mathcal{R}\Big/\left[1 + 2iQ\left(\frac{\omega_R - \omega_{RF} - is}{\omega_R}\right)\right],$$

$$= \mathcal{R}\Big/\left[1 + \frac{i(\omega_R - \omega_{RF} - is)}{\alpha}\right],$$

$$= \mathcal{R}\Big/\left(1 + \frac{s}{\alpha} + i\tan\phi_y\right), \tag{22}$$

where

$$\alpha = \frac{\omega_R}{2Q}, \tag{23}$$

ϕ_y is the detuning angle defined in Eq. (3), and the relation $\omega \approx \omega_s \ll h\Omega_0 = \omega_{RF}$ has been used. Similarly, we have

$$Z_{-h}(\omega - h\Omega_0) \approx \mathcal{R}\Big/\left(1 + \frac{s}{\alpha} - i\tan\phi_y\right). \tag{24}$$

Therefore,

$$\mathcal{Z}_-(\omega) = Z_h(\omega + h\Omega_0) - Z_{-h}(\omega - h\Omega_0),$$

$$\approx \frac{-2i\mathcal{R}\tan\phi_y}{\left(1 + \dfrac{s}{\alpha}\right)^2 + \tan^2\phi_y}. \tag{25}$$

Substituting Eqs. (12) and (15) together with the above expression into Eq. (21) yields

$$(s^2 + \omega_s^2)[(\alpha + s)^2 + \alpha^2\tan^2\phi_y] - \frac{K\alpha^2\omega_s^2 I_h \mathcal{R}\tan\phi_y}{V_m\cos\psi_s} = 0, \tag{26}$$

where

$$K = -\frac{4MR\omega_s qc\beta}{h^2 I_h}\int_0^\infty \frac{df_0}{dr}\left[J_1\left(\frac{hr}{R}\right)\right]^2 dr, \tag{27}$$

and $I_h \approx I_b$ is the Fourier component of the beam current at $\omega = \omega_{RF} = h\Omega_0$. Note that Eq. (26) is the same as Eq. (A.24) derived from the equivalent circuit approach in Appendix A except for the factor K in the last term. Also note that only the imaginary part of the resonator impedance was used in Eq. (21).

To proceed further, we rewrite Eq. (26) as

$$s^4 + a_3 s^3 + a_2 s^2 + a_1 s + a_0 = 0, \tag{28}$$

where

$$a_0 = \alpha^2\omega_s^2\left(\sec^2\phi_y - \frac{KI_h\mathcal{R}\tan\phi_y}{V_m\cos\phi_s}\right), \tag{29}$$

$$a_1 = 2\alpha\omega_s^2, \tag{30}$$

$$a_2 = \omega_s^2 + \alpha^2 \sec^2 \phi_y, \tag{31}$$

and

$$a_3 = 2\alpha. \tag{32}$$

The conditions for stability, by Routh's criterion,[26] are (i) $a_0 > 0$ and $a_3 > 0$, (ii) $a_2 a_3 - a_1 > 0$, and (iii) $a_1 a_2 a_3 - a_1^2 - a_0 a_3^2 > 0$. Condition (i) is satisfied if

$$\sec^2 \phi_y > \frac{K I_h \mathfrak{R} \tan \phi_y}{V_m \cos \psi_s},$$

that is

$$\sin(2\phi_y) < \frac{2 V_m \cos \psi_s}{K I_h \mathfrak{R}}. \tag{33}$$

Condition (ii) is always satisfied for obvious reasons. Under condition (i), one finds that condition (iii) is equivalent to

$$\tan \phi_y > 0. \tag{34}$$

Combining Eqs. (33) and (34), we have, for $\gamma < \gamma_t$, the stability conditions as

$$0 < \sin(2\phi_y) < \frac{2 V_m \cos \psi_s}{K I_h \mathfrak{R}}. \tag{35}$$

Except for the factor K, the stability conditions derived here are the same as the conditions in Inequalities (1) and (2). In terms of the averaged beam current I, the above conditions can be rewritten as

$$0 < \sin(2\phi_y) < \frac{2 V_m \cos \psi_s}{F_1 I \mathfrak{R}}, \tag{36}$$

where the *reduced form factor** F_m is defined as

$$F_m = \frac{4\int_0^\infty \frac{df_0}{dr}\left[J_m\left(\frac{hr}{R}\right)\right]^2 dr}{\frac{h^2}{R^2}\int_0^\infty f_0(r) r\, dr}. \tag{37}$$

Next, consider the quantity K and the reduced form factor F_1. The hth harmonic of the beam current is given by

$$\begin{aligned} I_h &= \frac{Mqc\beta}{2\pi}\int_0^{2\pi R}\int_{-\infty}^{\infty}[e^{ihz/R} + e^{-ihz/R}] f_0(z, v_z)\, dv_z\, dz, \\ &= \frac{Mqc\beta\omega_s}{2\pi R}\int_0^\infty\int_0^{2\pi} f_0(r)[e^{ihr\cos\phi/R} + e^{-ihr\cos\phi/R}]\, d\phi\, r\, dr, \\ &= \frac{2Mqc\beta\omega_s}{R}\int_0^\infty f_0(r) J_0\left(\frac{hr}{R}\right) r\, dr, \end{aligned} \tag{38}$$

* The term *form factor* was used in Ref. 5 for a different quantity.

where

$$\phi = \tan^{-1}(-v_z/\omega_s z),$$

is the phase of the synchrotron motion. Therefore,

$$K = \frac{2\int_0^\infty \frac{df_0}{dr}\left[J_1\left(\frac{hr}{R}\right)\right]^2 dr}{\frac{h^2}{R^2}\int_0^\infty f_0(r)J_0\left(\frac{hr}{R}\right)r\,dr} = \frac{F_1\int_0^\infty f_0(r)r\,dr}{2\int_0^\infty f_0(r)J_0\left(\frac{hr}{R}\right)r\,dr}. \tag{39}$$

3. DIPOLE-QUADRUPOLE MODE COUPLING

We now study the effect of the coupling between the dipole and quadrupole modes. To examine the dipole-quadrupole coupling effects, we have to include the modes of $l = \pm 2$, and $m = \pm 2$, also. In this case, we can derive the following four equations from Eq. (9):

$$(\omega - 2\omega_s)\Gamma_2 = -2i\vartheta_2[\mathscr{Z}_-(\Gamma_2 + \Gamma_{-2}) - i\mathscr{Z}_+(\Gamma_1 - \Gamma_{-1})], \tag{40}$$

$$(\omega - \omega_s)\Gamma_1 = -i\vartheta_1[i\mathscr{Z}_+(\Gamma_2 + \Gamma_{-2}) + \mathscr{Z}_-(\Gamma_1 - \Gamma_{-1})], \tag{41}$$

$$(\omega + \omega_s)\Gamma_{-1} = -i\vartheta_1[i\mathscr{Z}_+(\Gamma_2 + \Gamma_{-2}) + \mathscr{Z}_-(\Gamma_1 - \Gamma_{-1})], \tag{42}$$

and

$$(\omega + 2\omega_s)\Gamma_{-2} = -2i\vartheta_2[-\mathscr{Z}_-(\Gamma_2 + \Gamma_{-2}) + i\mathscr{Z}_+(\Gamma_1 - \Gamma_{-1})], \tag{43}$$

where Γ_m and ϑ_m are defined in Eqs. (13) and (15), respectively, $\mathscr{Z}_-$ has been given in Eq. (16) and

$$\mathscr{Z}_+ = \mathscr{Z}_+(\omega) = Z_h(\omega + h\Omega_0) + Z_{-h}(\omega - h\Omega_0). \tag{44}$$

Equating the determinant of the coefficients of Γ_2, Γ_1, Γ_{-1}, and Γ_{-2} to zero and making a change of variable from ω to s yields the dispersion relation

$$s^6 + b_5 s^5 + b_4 s^4 + b_3 s^3 + b_2 s^2 + b_1 s + b_0 = 0, \tag{45}$$

where

$$b_0 = 4\alpha^2\omega_s^2[\omega_s^2 \sec^2\phi_y + 16\mathscr{R}^2\vartheta_1\vartheta_2 - 4\mathscr{R}\omega_s(\vartheta_1 + \vartheta_2)\tan\phi_y], \tag{46}$$

$$b_1 = 8\alpha\omega_s^4, \tag{47}$$

$$b_2 = 4\omega_s^4 + 5\omega_s^2\alpha^2\sec^2\phi_y - 4\mathscr{R}\omega_s\alpha^2(\vartheta_1 + 4\vartheta_2)\tan\phi_y, \tag{48}$$

$$b_3 = 10\alpha\omega_s^2, \tag{49}$$

$$b_4 = 5\omega_s^2 + \alpha^2\sec^2\phi_y, \tag{50}$$

and

$$b_5 = 2\alpha. \tag{51}$$

In arriving at Eq. (45), we have used the approximations for the resonator impedance in Eqs. (22) and (24).

By Routh's criterion, the conditions for stability are (i) $b_5 > 0$, (ii) $b_4 b_5 - b_3 > 0$,

(iii) $v_1 > 0$, (iv) $w_1 > 0$, (v) $v_2 - \frac{b_0 v_1}{w_1} > 0$, and (vi) $b_0 > 0$, where

$$v_1 = b_3 - b_5\left(\frac{b_5 b_2 - b_1}{b_4 b_5 - b_3}\right), \tag{52}$$

$$v_2 = b_1 - \left(\frac{b_0 b_5^2}{b_4 b_5 - b_3}\right), \tag{53}$$

and

$$w_1 = b_2 - \frac{b_1}{b_5} - \left(\frac{v_2}{v_1}\right)\left(b_4 - \frac{b_3}{b_5}\right). \tag{54}$$

It is straightforward to prove that Conditions (i) and (ii) are always satisfied. Condition (iii) can be simplified to the requirement of

$$\tan \phi_y > 0. \tag{55}$$

Under Condition (iii), one can show that Condition (iv) can be satisfied if

$$16\mathscr{R}\vartheta_1\vartheta_2 + \omega_s(\vartheta_1 + 16\vartheta_2)\tan\phi_y - 4\mathscr{R}(\vartheta_1 + 4\vartheta_2)^2 \sin^2\phi_y > 0. \tag{56}$$

Assuming Condition (iv) is satisfied, then Condition (v) is equivalent to

$$4\alpha^2\omega_s^4[16\mathscr{R}\vartheta_1\vartheta_2 + \omega_s(\vartheta_1 + 16\vartheta_2)\tan\phi_y - 4\mathscr{R}(\vartheta_1 + 4\vartheta_2)^2\sin^2\phi_y] > b_0[\omega_s(\vartheta_1 + 16\vartheta_2)\tan\phi_y + 16\mathscr{R}\vartheta_1\vartheta_2]\cos^2\phi_y, \tag{57}$$

which can be simplified to

$$\left(\tan\phi_y - \frac{16\mathscr{R}\vartheta_2}{3\omega_s}\right)\left(\tan\phi_y + \frac{4\mathscr{R}\vartheta_1}{3\omega_s}\right) > 0,$$

or

$$\tan\phi_y > \frac{16\mathscr{R}\vartheta_2}{3\omega_s}. \tag{58}$$

Thus, Inequalities (57) and (58) describe the same condition. If Condition (vi) is satisfied, one will find that Inequalities (57) and (58) are more restrictive than Inequalities (55) and (56); that is, if $b_0 > 0$ and the condition in Inequality (57) or (58) is satisfied, then Inequalities (55) and (56) are also satisfied. Condition (vi) can be shown to be the same as the inequality

$$\left(\tan\phi_y - \frac{4\mathscr{R}\vartheta_1}{\omega_s}\right)\left(\tan\phi_y - \frac{4\mathscr{R}\vartheta_2}{\omega_s}\right) + 1 > 0. \tag{59}$$

Combining Inequalities (58) and (59), we can infer the following stability conditions: (for $\gamma < \gamma_t$)

[1] If $\sin\phi_y \le [2\sqrt{\xi}/(1+\xi)]$, then

$$I < \frac{3\tan\phi_y V_m \cos\psi_s}{4F_2\mathscr{R}} = I_d T_3, \tag{60}$$

where I is the averaged beam current,

$$I_d = \frac{2V_m \cos \psi_s}{F_1 \mathcal{R} \sin(2\phi_y)}, \tag{61}$$

is the maximum stable current for the dipole mode for no coupling with the quadrupole mode,

$$T_3 = \frac{3 \sin^2 \phi_y}{4\xi}, \tag{62}$$

and

$$\xi = \frac{F_2}{F_1}. \tag{63}$$

Note that in this region,

$$0 \le T_3 \le \frac{3}{(1+\xi)^2}.$$

[2] For $[2\sqrt{\xi}/(1+\xi)] \le \sin \phi_y \le [4\sqrt{\xi/(3+12\xi)}]$, there are two subcases:
(a) for $1/2 \le \xi$:

$$I < I_d T_3, \tag{64}$$

where

$$\frac{3}{(1+\xi)^2} \le T_3 \le \frac{4}{1+4\xi},$$

and **(b)** for $\xi \le 1/2$, there are two stable regions:

$$I < I_d T_1, \tag{65}$$

and

$$I_d T_2 < I < I_d T_3, \tag{66}$$

where

$$T_1 = \left(\frac{\sin^2 \phi_y}{2\xi}\right)\left[1 + \xi - \sqrt{(1-\xi)^2 - 4\xi \cot^2 \phi_y}\right], \tag{67}$$

and

$$T_2 = \left(\frac{\sin^2 \phi_y}{2\xi}\right)\left[1 + \xi + \sqrt{(1-\xi)^2 - 4\xi \cot^2 \phi_y}\right]. \tag{68}$$

In this subcase

$$\frac{4}{3} \le T_1 \le \frac{2}{1+\xi},$$

$$\frac{2}{1+\xi} \le T_2 \le \frac{4}{1+4\xi},$$

and

$$\frac{3}{(1+\xi)^2} \le T_3 \le \frac{4}{1+4\xi}.$$

Note that when $\xi = 1/2$,

$$\frac{2}{1+\xi} = \frac{4}{1+4\xi} = \frac{3}{(1+\xi)^2} = \frac{4}{3}.$$

[3] If $[4\sqrt{\xi}/(3+12\xi)] \leq \sin \phi_y$, then

$$I < I_d T_1, \tag{69}$$

where

$$1 \leq T_1 \leq \frac{4}{3}, \qquad \text{for } \xi \leq \frac{1}{2},$$

and

$$1 \leq T_1 \leq \frac{4}{1+4\xi}, \qquad \text{for } \xi \geq \frac{1}{2}.$$

In most practical situations, $\xi < (1/2)$ and $[2\sqrt{\xi}/(1+\xi)] < \sin \phi_y$, so the condition described in Inequalities (65) and (69) corresponds to the limit of the beam current in the majority of practical cases. It can be shown that when $\xi \cot^2 \phi_y$ is very small, the stability condition in Inequalities (65) and (69) reduces to

$$I < I_d(1 + \xi \cot^2 \phi_y). \tag{70}$$

When $\vartheta_2 = 0$ or $\xi = 0$, the above condition and Inequality (58) are the same as Inequality (36).

4. NUMERICAL RESULTS AND DISCUSSIONS

Examples of the reduced form factors F_1 and F_2 as well as the quantities K and ξ are given in Appendix B as functions of g for several equilibrium distribution functions, where the parameter g is related to the full bunch length L and the bunching factor B by

$$g = \frac{hL}{2R} = \pi B. \tag{71}$$

The reduced form factors F_1 and F_2 as functions of g are plotted in Figs. 1 and 2, respectively, for the distribution functions treated in Appendix B. Numerical results for the quantities K and ξ are shown in Figs. 3 and 4, respectively. For our discussions, it is sufficient to show the values of these quantities from $g = 0$ up to $g = 1.5$. Beyond $g = 1.5$, the linear approximation for the longitudinal focusing force may be inadequate. All the curves in these figures show a common property: in each figure, curves corresponding to different equilibrium distribution functions all converge when the value of g approaches zero. When g is equal to zero, F_1 has a value of 2, F_2 is equal to zero, K is equal to one, and ξ is equal to zero. The behavior of the quantity K is similar to that of the reduced form factor F_1. When g or the bunch length increases, the values of F_1 and K decrease, thereby suggesting that the dipole mode is more stable in a long bunch than in a

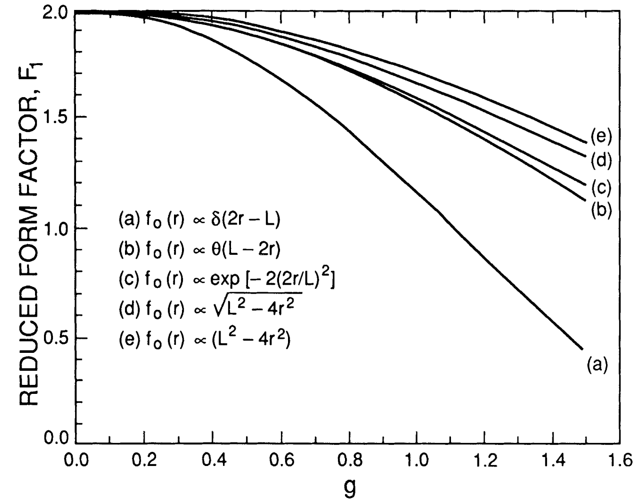

FIGURE 1 The reduced form factor F_1 as a function of the parameter g for the equilibrium distribution functions considered in Appendix B.

short bunch. Because K has the maximal value of 1, Eq. (35) indicates that the threshold current of the dipole mode, derived from the Vlasov equation, could be higher than Robinson's limit in Eq. (2). The decreased separations among the curves in Figure 1 and 3 as the g value decreased implies that for short bunches, the difference between phase-space distributions has little effect on the stability of the dipole mode. Fig. 4 shows that the value of ξ is normally much smaller than one, except for very long bunches or beams with delta-function distribution in the amplitude of synchrotron oscillation.

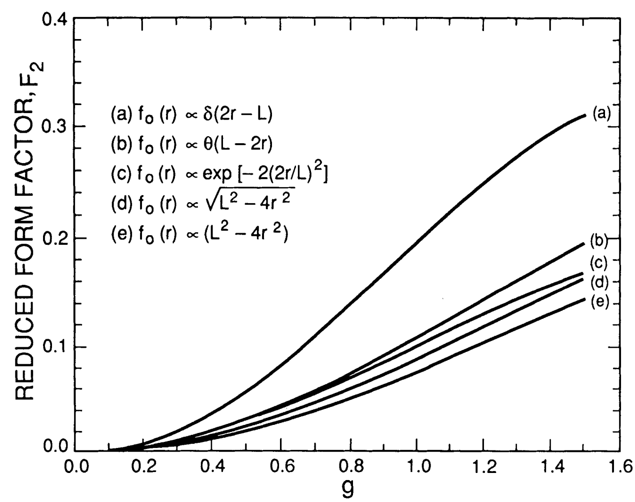

FIGURE 2 The reduced form factor F_2 as a function of the parameter g for the equilibrium distribution functions considered in Appendix B.

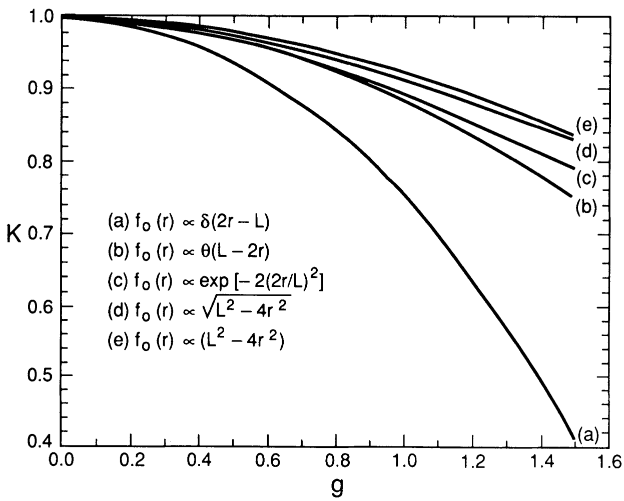

FIGURE 3 The values of the factor K as a function of g for the equilibrium distribution functions considered in Appendix B.

The quantities T_1, T_2, and T_3 represent the ratios between the maximum stable beam current with quadrupole-dipole mode coupling and the maximum stable beam current for dipole mode perturbation only; hence, their numerical values are interesting to us. The discussions in the last section have shown that only T_3 can have values less than one, and it happens only when $3\sin^2\phi_y < 4\xi$. Thus, if one can manage to have $3\sin^2\phi_y > 4\xi$, then the maximum stable current can be higher than that predicted by Robinson's critiera. We note that the maximal values of T_2 and T_3 can be as large as four. The numerical values of T_1, T_2, and T_3

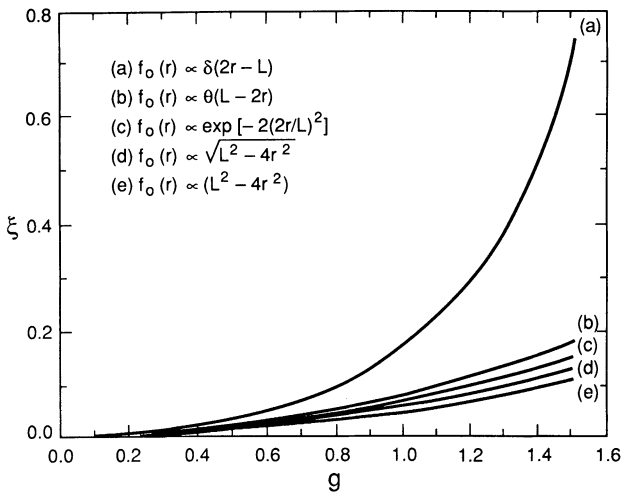

FIGURE 4 The quantity ξ as a function of g for the equilibrium distribution functions considered in Appendix B.

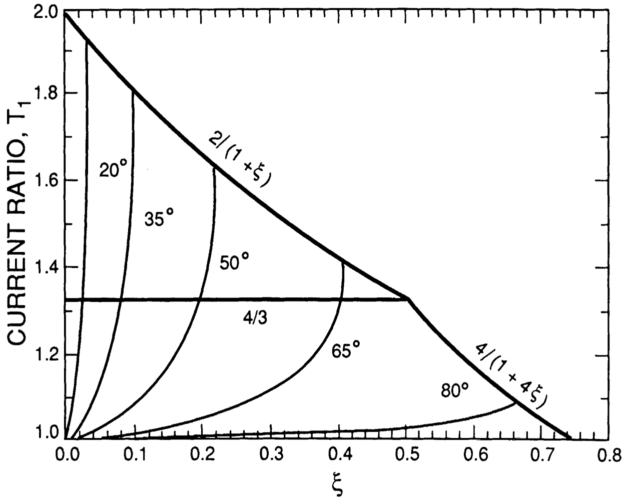

FIGURE 5 The *current ratio* T_1 as a function of ξ for various values of the detuning angle ϕ_y. Thick curves correspond to the extreme values of T_1 discussed in the text.

are shown in Figs. 5 to 7 as functions of ξ for various values of the detuning angle ϕ_y. As can be seen in the figures, the highest current ratios are all in the regions of small ξ and small cavity detuning. It may be worthwhile to recall here that cavity detuning is necessary because finite rf power is used for acceleration or bunching, and also that the required phase between the total voltage on the cavity and beam current is maintained by compensating the beam-load with rf power. Therefore, in most cases, smaller cavity detuning implies higher cavity voltage so that the power consumption is higher than minimally required. As shown in the figures, the value of the parameter ξ increases with bunch length and, therefore,

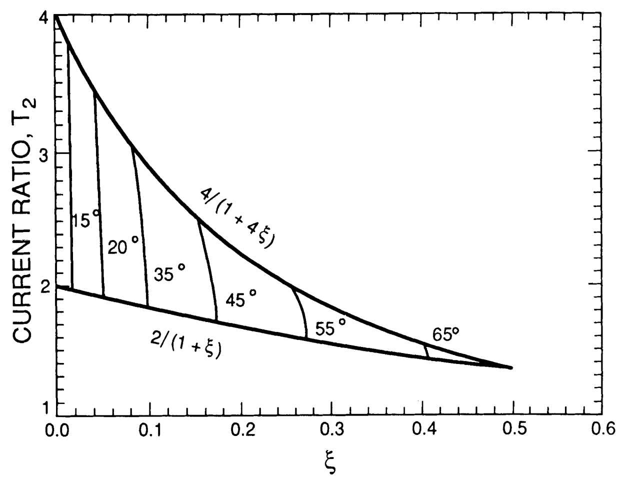

FIGURE 6 The *current ratio* T_2 as a function of ξ for various values of the detuning angle ϕ_y. Thick curves correspond to the extreme values of T_2 considered in the text.

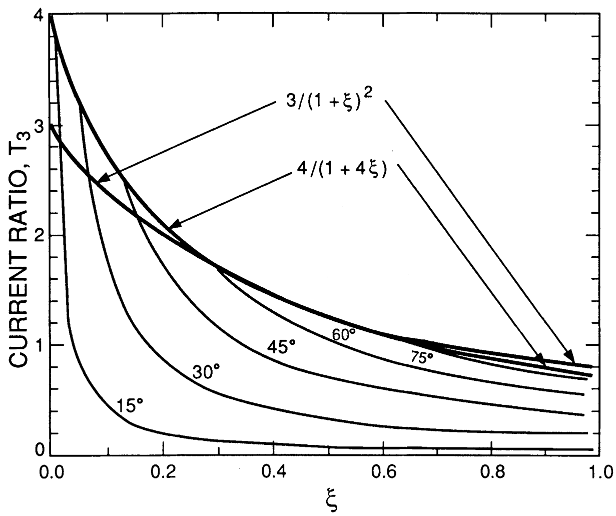

FIGURE 7 The *current ratio* T_3 as a function of ξ for various values of the detuning angle ϕ_y. Thick curves correspond to the extreme values of T_3 considered in the text.

the values of T_2 and T_3 decrease with bunch length. This means that in the small detuning region, the coupling between dipole and quadrupole modes makes long bunches more unstable than short bunches. Figure 8 shows the ratio between the threshold current with dipole-quadrupole coupling I_{dq} and the threshold current of the dipole mode I_d as a function of the cavity detuning angle ϕ_y for various values of ξ. The small stable regions of $T_2 < (I/I_d) < T_3$ have been neglected in the figure. The ratio I_{dq}/I_d has a maximal value of $3/(1+\xi)^2$ at $\sin\phi_y = 2\sqrt{\xi}/(1+\xi)$. The values of I_{dq}/I_d on the left-hand side and the

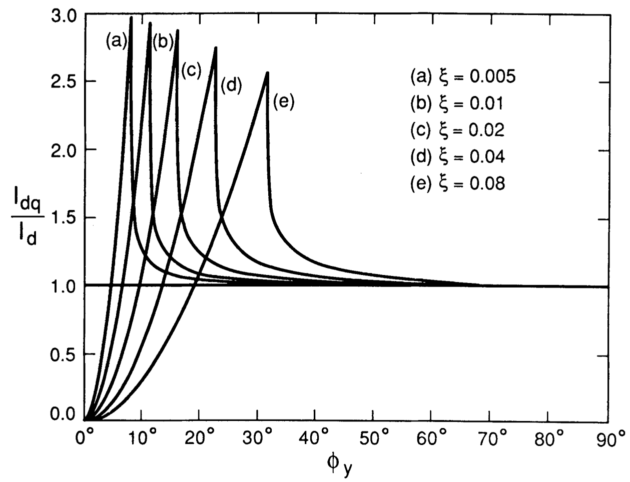

FIGURE 8 The ratio between the threshold current with dipole-quadrupole coupling I_{dq} and the dipole mode threshold current I_d is shown as a function of the detuning angle ϕ_y for some values of ξ. In the figure, we have neglected the small stable regions of $T_2 < (I/I_d) < T_3$.

right-hand side of the peak are given by the values of T_3 and T_1, respectively. The peak has small width and large height at small values of ξ. When the value of ξ increases, the height drops, but the width increases. For $\sin \phi_y > 2\sqrt{\xi}/(1+\xi)$, I_{dq} decreases to I_d as a limit when the detuning angle approaches 90°. For $\sin \phi_y < 2\sqrt{\xi}/(1+\xi)$, I_{dq} falls off like $\tan \phi_y/\xi$, as described in Eq. (60). Thus, in the small cavity detuning region, Robinson's criterion is significantly modified by the coupling with the quadrupole mode. To conclude our results here, we emphasize that the stability limits shown in Fig. 8 are qualitatively in agreement with recent computer simulations[27] that include synchrotron harmonics higher than the quadrupole mode.

5. CONCLUSION

We have shown that the stability criteria that Robinson derived previously using an equivalent circuit model agrees very well with that obtained from the Vlasov equation in the kinetic description. We found that the stability threshold current of the dipole mode derived from the Vlasov equation is higher than Robinson's limit, particularly in a long bunch. We have also studied the coupling between the dipole and quadrupole modes under the influence of a resonator impedance. For small cavity detuning. Robinson's stability limit is substantially modified by the coupling between the dipole mode and the quadrupole mode.

ACKNOWLEDGMENT

The author would like to thank R. K. Cooper for his reading of the manuscript and his comments as well as his encouragement. He would like also to thank A. Hofmann, F. Pederson, B. Zotter, G. Rees for their comments and H. A. Thiessen for his encouragement.

REFERENCES

1. K. W. Robinson, "Radiofrequency Acceleration II," Cambridge Electron Accelerator, report CEA-11, Cambridge, Mass. (1956).
2. K. W. Robinson, "Stability of Beam in Radio-Frequency Systems," Cambridge Electron Accelerator, report CEAL-1010, Cambridge, Mass. (1964).
3. A. N. Lebedev, *At. Energ.* [*Sov. J. At. Energy*], **25,** 100 (1968). (English translation, p. 851.)
4. F. J. Sacherer, "Method for Computing Bunched-Beam Instabilities," CERN internal report CERN/SI-BR/72-5 (1972).
5. F. J. Sacherer, "Bunch Lengthening and Microwave Instability," *IEEE Trans. Nucl. Sci.* **24,** 1393 (1977).
6. F. J. Sacherer, "Bunch Lengthening and Microwave Instability," CERN internal report CERN/PS/BR 77-6 (1977).
7. I. G. Henry, "Phase Oscillations in High Current Synchrotrons," *J. Appl. Phys.* **31,** 1338 (1960).
8. A. I. Baryshev and S. A. Kheifets, *Sov. Phys. Tech. Phys.* **8,** 235 (1964).
9. M. M. Karliner, A. N. Skrinskii, and I. A. Shekhtman, *Sov. Phys. Tech. Phys.* **13,** 1560 (1969).
10. I. Gumoski, "Stability of Coherent Synchrotron Motion, Part I," CERN internal report CERN/SI/INT./DL/70-13 (1970).

11. I. Gumoski, "Stability of Coherent Synchrotron Motion, Part II," CERN Internal report CERN/SI/INT./DL/71-6 (1971).
12. M. Sands, "Beam-Cavity Interaction-I: Basic Considerations," *rapport technique* 2-76, and "Beam-Cavity Interaction-II: Maximum Beam Current," *rapport technique* 3-76, Laboratoire de l'Accélérateur Linéare, Orsay (1976).
13. A. Hofmann, lecture note in "*Theoretical Aspects of the Behaviour of Beams in Accelerators and Storage Rings,*" CERN report 77–13, p. 163 (1977).
14. É. A. Myaé, P. T. Pashkov, and A. V. Smirnov, *Sov. Phys. Tech. Phys.* **26,** 42 (1981).
15. P. B. Wilson and J. E. Griffin, "High Energy Electron Linacs; Application to Storage Ring RF Systems and Linear Colliders," in: *Physics of High Energy Particle Accelerators,* R. A. Carrigan, F. R. Huson, and M. Month, eds. American Institute of Physics Conf. Proc. **87** (1982).
16. P. T. Pashkov and A. V. Smirnov, *At. Energy.* [*Sov. J. At. Energy*], **50,** 408 (1981). (English translation p. 372.)
17. T. Suzuki and K. Yokoya, *Nucl. Instrum. Meth.* **203,** 45 (1982).
18. H. Nishimura, *Jpn. J. Appl. Phys.* **22,** 518 (1983).
19. A. W. Chao, "Stability of the Higher Order Longitudinal Modes for PEP," Stanford Linear Accelerator Center PEP Note 309, (1979).
20. É. A. Myaé, P. T. Pashkov, and A. V. Smirnov, *Sov. Phys. Tech. Phys.* **25** (6), 713 (1980).
21. B. Zotter, "Longitudinal Stability of Bunched Beams, Part I: Resonator Impedances," CERN internal report CERN SPS/81–18 (1981).
22. T. Suzuki, Y. Chin, and K. Satoh, *Part. Accel.* **13,** 179 (1983).
23. G. H. Rees, "Another Look at Coherent Longitudinal Instability of Bunched Beams," Proc. First European Particle Accelerator Conf., Rome, July 1988 (to be published).
24. S. R. Koscielniak, "Computer Simulations of Beam Loading," TRIUMF Design Note TRI-DN-88-34 (1988).
25. T. Suzuki, *Part. Accel.* **12,** 237 (1982).
26. E. J. Routh, *A Treatise on the Dynamics of a System of Rigid Bodies,* (Macmillan, London, 1877).
27. See Figs. 5c and 6 in Ref. 24.
28. For example, see Ref. 1 and "RF Stability for the PSR," by R. K. Cooper and P. L. Morton, PSR Technical Note #17, Accelerator Technology Division, Los Alamos National Laboratory (1978).

APPENDIX A

Equivalent Circuit Derivation

The equivalent circuit model was originally adopted by K. W. Robinson.[1,2] In this approach, the linearization of the circuit equations is usually performed geometrically by using phasor diagrams.[28] The following derivation uses an algebraic linearization procedure that will give us the same results. We will concentrate on the case of $\gamma < \gamma_t$. The case of $\gamma > \gamma_t$ can be treated by the same procedures.

In the equivalent circuit model, a cavity is envisioned as a parallel RLC circuit; the applied rf power source and the circulating beam current are envisioned as currents i_g and i_b, respectively. The schematic is shown in Fig. A-1.

Using Kirchhoff's law, one can derive that the total voltage on the cavity satisfies the differential equation

$$\frac{d^2v}{dt^2} + 2\alpha\frac{dv}{dt} + \omega_R^2 v = 2\alpha\mathcal{R}\frac{di_t}{dt}, \tag{A.1}$$

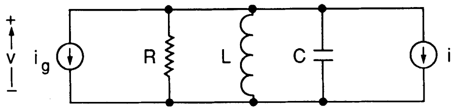

FIGURE A-1 The equivalent circuit model of the beam-cavity interaction system.

where v is the total voltage, α has been defined in Eq. (23), and

$$i_t = i_g + i_b. \tag{A.2}$$

Making the substitutions of

$$v = \tilde{V}(t)e^{-i\omega_g t}, \tag{A.3}$$

$$i_g = \tilde{I}_g(t)e^{-i\omega_g t}, \tag{A.4}$$

and

$$i_b = \tilde{I}_b(t)e^{-i\omega_g t}, \tag{A.5}$$

in Eq. (A.1) yields

$$\frac{d^2\tilde{V}}{dt^2} + 2(\alpha - i\omega_g)\frac{d\tilde{V}}{dt} + (\omega_R^2 - \omega_g^2 - 2i\alpha\omega_g)\tilde{V} = 2\alpha\mathscr{R}\left(\frac{d\tilde{I}}{dt} - i\omega_g\tilde{I}\right), \tag{A.6}$$

where $\omega_g = \omega_{RF} = h\Omega_0$ is the frequency of the driving rf power and

$$\tilde{I} = \tilde{I}_g - \tilde{I}_b. \tag{A.7}$$

For high-Q and high-frequency resonators, $\alpha \ll \omega_g$, and $d^2\tilde{V}/dt^2 \ll \omega_g d\tilde{V}/dt$. If we also assume that $d\tilde{I}/dt \ll \omega_g\tilde{I}$, which is true in general, Eq. (A.6) can be approximated by

$$\frac{d\tilde{V}}{dt} + \left[\alpha - \frac{i(\omega_g^2 - \omega_R^2)}{2\omega_g}\right]\tilde{V} = \alpha\mathscr{R}\tilde{I}. \tag{A.8}$$

The relations among these phasors are shown in Fig. A-2, where we have chosen a rotating polar coordinate system such that the steady state $\tilde{I}_b$ is on the real axis.

For the system under consideration, the phasors will oscillate with respect to their steady state. We shall use ϕ_v and ϕ_b to denote the angular deviations of $\tilde{V}$ and $\tilde{I}_b$ from their steady states, respectively.

Using the notations defined above, we can write the phasors in polar form as:

$$\tilde{I}_b = I_b(t)e^{-i\phi_b(t)}, \tag{A.9}$$

$$\tilde{I}_g = I_g(t)e^{-i\psi_g}, \tag{A.10}$$

and

$$\tilde{V} = V(t)e^{-i\psi_v - i\phi_v(t)}. \tag{A.11}$$

Substituting the above polar representations into Eq. (A.8) and equating the real and imaginary parts on both sides of the equality, we have

$$\frac{dV}{dt} + \alpha V = \alpha\mathscr{R}[-I_b\cos(\phi_b - \phi_v - \psi_v) + I_g\cos(\phi_v - \psi_g + \psi_v)], \tag{A.12}$$

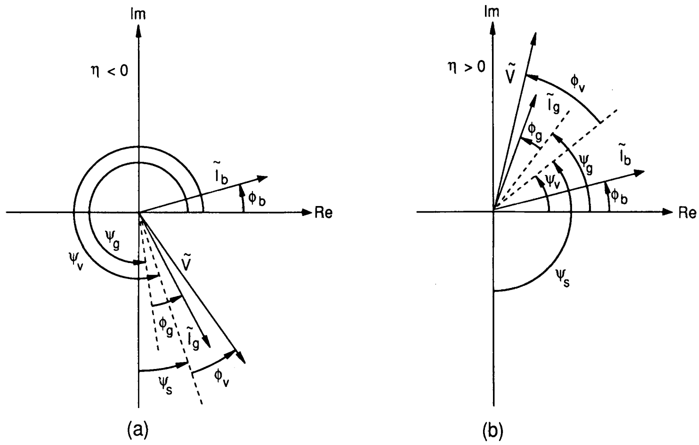

FIGURE A-2 Phasor diagram showing the relations among the beam current, $\tilde{I}_b$, the generator current, $\tilde{I}_g$, and the total cavity voltage, $\tilde{V}$, for (a) $\gamma < \gamma_t$ and (b) $\gamma > \gamma_t$; ψ_s represents the synchronous angle and the dashed lines designate steady-state angles.

and

$$\frac{d\phi_v}{dt} = \omega_R - \omega_g - \frac{\alpha\mathcal{R}}{V}[I_b \sin(\phi_b - \phi_v - \psi_v) + I_g \sin(\phi_v - \psi_g + \psi_v)], \quad \text{(A.13)}$$

where use has been made of the approximation $\omega + \omega_R \approx 2\omega$.

One can prove that when $\psi_g = \psi_v$, the system will be in tune, that is, the rf source will see a *real* impedance. In this case, Eqs. (A.12) and (A.13) are simplified to

$$\frac{dV}{dt} + \alpha V = \alpha\mathcal{R}[-I_b \cos(\phi_b - \phi_v - \psi_v) + I_g \cos\phi_v], \quad \text{(A.14)}$$

and

$$\frac{d\phi_v}{dt} = \omega_R - \omega_g - \frac{\alpha\mathcal{R}}{V}[I_b \sin(\phi_b - \phi_v - \psi_v) + I_g \sin\phi_v]. \quad \text{(A.15)}$$

The subsequent analysis will always assume that the system is in tune. Notice that the total voltage in the steady state V_s is given by

$$V_s = \mathcal{R}(I_g - I_b \cos\psi_v). \quad \text{(A.16)}$$

Also note that in the steady state,

$$\frac{\mathcal{R}I_b \sin\psi_v}{V_s} = -\frac{\omega_R - \omega_g}{\alpha} = -\tan\phi_y. \quad \text{(A.17)}$$

The equations of beam motion are given by the equations of synchrotron motion:

$$\frac{d\Delta E}{dt} = \frac{\alpha\omega_g}{2\pi h}[V \sin(\psi_s + \phi_v - \phi_b) - V_s \sin\psi_s], \quad \text{(A.18)}$$

and

$$\frac{d\phi_b}{dt} = -\frac{\eta\omega_g}{\beta^2}\left(\frac{\Delta E}{E_0}\right), \tag{A.19}$$

where E_0 is the total energy of the reference particle, ΔE is the energy deviation from E_0, and η has been defined in Eq. (5). Assuming that I_b is constant and a small perturbation $\hat{V}$ is introduced to the voltage, one can linearize Eqs. (A.14), (A.15), (A.18), and (A.19) to yield

$$\frac{d\hat{V}}{dt} + \alpha\hat{V} = -\alpha\mathcal{R}I_b(\phi_b - \phi_v)\sin\psi_v, \tag{A.20}$$

$$\frac{d\phi_v}{dt} + \alpha\phi_v = -\frac{\alpha\mathcal{R}I_b\hat{V}\sin\psi_v}{V_s^2} - \frac{\alpha\mathcal{R}I_b\phi_b\cos\psi_v}{V_s}, \tag{A.21}$$

and

$$\frac{d}{dt}\left(\frac{\Delta E}{E_0}\right) = \frac{q\omega_g}{2\pi hE_0}[V_s(\phi_v - \phi_b)\cos\psi_s + \hat{V}\sin\psi_s]. \tag{A.22}$$

Making the substitutions of $\hat{V} = \bar{V}e^{st}$, $\Delta E = \bar{E}e^{st}$, $\phi_v = \bar{\phi}_v e^{st}$, and $\phi_b = \bar{\phi}_b e^{st}$ in Eqs. (A.19) to (A.22), then using the relations $\sin\psi_v = -\cos\psi_s$, $\cos\psi_s = \sin\psi_s$, and Eq. (A.17), we can derive that

$$\begin{pmatrix} s+\alpha & \alpha V_s\tan\phi_y & 0 & -\alpha\mathcal{R}I_b\cos\psi_s \\ -\dfrac{\alpha\tan\phi_y}{V_s} & s+\alpha & 0 & \dfrac{\alpha\mathcal{R}I_b\sin\psi_s}{V_s} \\ \dfrac{q\omega_g\sin\psi_s}{2\pi hE_0} & \dfrac{q\omega_g V_s\cos\psi_s}{2\pi hE_0} & -s & \dfrac{-q\omega_g V_s\cos\psi_s}{2\pi hE_0} \\ 0 & 0 & -\dfrac{\eta\omega_g}{\beta^2} & -s \end{pmatrix} \begin{pmatrix} \bar{V} \\ \bar{\phi}_v \\ \dfrac{\bar{E}}{E_0} \\ \bar{\phi}_b \end{pmatrix} = 0. \tag{A.23}$$

In order to have nontrivial solutions for $\bar{V}$, $\bar{\phi}_v$, $\bar{E}$, and $\bar{\phi}_b$, the determinant of Eq. (A.23) must be zero. We therefore have

$$(s^2 + \omega_s^2)[(s+\alpha)^2 + \alpha^2\tan^2\phi_y] - \frac{\alpha^2\omega_s^2\mathcal{R}I_b\tan\phi_y}{V_s\cos\psi_s} = 0. \tag{A.24}$$

Equation (A.24) is the same as Eq. (26) derived from Sacherer's integral equation except for the factor K in the last term in Eq. (26). By identifying V_s as V_m, the maximum voltage on the rf cavity, and applying Routh's criterion, we obtain the stability conditions in Eqs. (1) and (2).

APPENDIX B

Examples of F_1, F_2, K and ξ

In Appendix B, we shall present examples of the reduced form factors F_1 and F_2 as well as the quantities K and ξ for some equilibrium distribution functions.

These quantities will be given as functions of the parameter g defined according to

$$g = \frac{hL}{2R}, \tag{B.1}$$

where L is the bunch length, h is the rf harmonic number and R is the effective machine radius.
[1] $f_0(r) \propto \delta(2r - L)$:

$$F_1 = \frac{8J_1(g)}{g}\left[J_0(g) - \frac{J_1(g)}{g}\right], \tag{B.2}$$

$$F_2 = \frac{8J_2(g)}{g}\left[J_1(g) - \frac{2J_2(g)}{g}\right], \tag{B.3}$$

$$K = \frac{4J_1(g)}{g}\left[1 - \frac{J_1(g)}{gJ_0(g)}\right], \tag{B.4}$$

and

$$\xi = \frac{J_2(g)}{J_1(g)}\left[\frac{gJ_1(g) - 2J_2(g)}{gJ_0(g) - J_1(g)}\right], \tag{B.5}$$

[2] $f_0(r) \propto \theta(L - 2r)$:

$$F_1 = \frac{8J_1^2(g)}{g^2}, \tag{B.6}$$

$$F_2 = \frac{8J_2^2(g)}{g^2}, \tag{B.7}$$

$$K = \frac{2J_1(g)}{g}, \tag{B.8}$$

and

$$\xi = \left[\frac{J_2(g)}{J_1(g)}\right]^2, \tag{B.9}$$

where $\theta(x)$ is the step function.
[3] $f_0(r) \propto \exp[-2(2r/L)^2]$:

$$F_1 = \frac{16}{g^2} I_1\left(\frac{g^2}{4}\right) \exp(-g^2/4), \tag{B.10}$$

$$F_2 = \frac{16}{g^2} I_2(g^2/4) \exp(-g^2/4), \tag{B.11}$$

$$K = \frac{8}{g^2} I_1\left(\frac{g^2}{4}\right) \exp(-g^2/8), \tag{B.12}$$

and

$$\xi = \frac{I_2(g^2/4)}{I_1(g^2/4)}, \tag{B.13}$$

where $I_1(x)$ and $I_2(x)$ are the modified Bessel functions of the first kind. Note that we have taken four standard deviations of the distribution as the bunch length.

[4] $f_0(r) \propto \sqrt{L^2 - 4r^2}$:

$$F_1 = 2\left(1 - \frac{g^2}{5} + \frac{g^4}{46} - \frac{g^6}{1890}\right), \tag{B.14}$$

$$F_2 = \frac{g^2}{10}\left(1 - \frac{g^2}{7} + \frac{7g^4}{828} - \frac{7g^6}{9108}\right), \tag{B.15}$$

$$K = \frac{g^3}{3}\left(1 - \frac{g^2}{5} + \frac{g^4}{46} - \frac{g^6}{1890}\right) \Big/ (\sin g - g\cos g), \tag{B.16}$$

and

$$\xi = \frac{g^2}{20}\left(1 - \frac{g^2}{7} + \frac{7g^4}{828} - \frac{7g^6}{9108}\right) \Big/ \left(1 - \frac{g^2}{5} + \frac{g^4}{46} - \frac{g^6}{1890}\right). \tag{B.17}$$

In obtaining the above results, we have expanded the Bessel functions $J_1(r)$ and $J_2(r)$ in Eq. (37) and kept the four lowest order terms. For $r \le 1.5$, the result should be accurate to 10^{-3}.

[5] $f_0(r) \propto (L^2 - 4r^2)$:

$$F_1 = \frac{16}{g^2}[J_1^2(g) - J_0(g)J_2(g)], \tag{B.18}$$

$$F_2 = \frac{16}{g^2}\left[J_1^2(g) + J_2^2(g) - \frac{4J_1(g)J_2(g)}{g}\right], \tag{B.19}$$

$$K = \frac{J_1^2(g)}{J_2(g)} - J_0(g), \tag{B.20}$$

and

$$\xi = \frac{g[J_1^2(g) + J_2^2(g)] - 4J_1(g)J_2(g)}{g[J_1^2(g) - J_0(g)J_2(g)]}. \tag{B.21}$$